

Article

Not peer-reviewed version

Ultrasound-Assisted Atomization Delivery System Improves the Uniformity of Nanoparticle Distribution in the Mucus Barrier

[Yunhao Li](#) and Rafael Torres *

Posted Date: 25 November 2025

doi: 10.20944/preprints202511.1822.v1

Keywords: ultrasonic nebulizer; droplet size; aerosol delivery; nanoparticle transport; mucus penetration; lung deposition; inhaled therapy



Preprints.org is a free multidisciplinary platform providing preprint service that is dedicated to making early versions of research outputs permanently available and citable. Preprints posted at Preprints.org appear in Web of Science, Crossref, Google Scholar, Scilit, Europe PMC.

Copyright: This open access article is published under a [Creative Commons CC BY 4.0 license](#), which permit the free download, distribution, and reuse, provided that the author and preprint are cited in any reuse.

Disclaimer/Publisher's Note: The statements, opinions, and data contained in all publications are solely those of the individual author(s) and contributor(s) and not of MDPI and/or the editor(s). MDPI and/or the editor(s) disclaim responsibility for any injury to people or property resulting from any ideas, methods, instructions, or products referred to in the content.

Article

Ultrasound-Assisted Atomization Delivery System Improves the Uniformity of Nanoparticle Distribution in the Mucus Barrier

Yunhao Li and Rafael Torres *

School of Chemical and Biomolecular Engineering, The University of Sydney, Sydney, NSW 2006, Australia

* Correspondence: r.torres@sydney.edu.au

Abstract

This study examined how ultrasonic frequency changes droplet size and affects the delivery of nanoparticles through airway mucus. A simple nebulizer system was tested at 1.7 MHz and 2.5 MHz using fluorescent nanoparticles in a mouse model. At 2.5 MHz, the average droplet size decreased from 4.5 μm to 2.1 μm , which increased total lung deposition by 38% and extended mucus penetration by about 25 μm . Fluorescence imaging showed that the higher frequency produced a more uniform spread and higher drug level in the alveolar region. These findings show that adjusting ultrasonic frequency can improve droplet control and nanoparticle movement in the lungs. This approach offers a useful way to improve inhaled drug delivery and may also support future aerosol treatments for long-term lung diseases.

Keywords: ultrasonic nebulizer; droplet size; aerosol delivery; nanoparticle transport; mucus penetration; lung deposition; inhaled therapy

1. Introduction

Aerosol delivery provides an effective therapeutic route for lung diseases by enabling localized administration while reducing systemic exposure and minimizing off-target toxicity [1]. Inhaled nanoparticles can improve drug residence in deep lung regions due to their favorable aerodynamic properties; however, their transport is strongly hindered by the airway mucus barrier [2]. This mucus layer, consisting of entangled mucins, salts, and cellular debris, forms a steric and adhesive obstacle that significantly limits nanoparticle diffusion and reduces access to underlying epithelial tissues. Recent studies have further highlighted that large aerosol droplets often result in non-uniform deposition, whereas well-regulated aerosolization enables more homogeneous distribution and deeper lung penetration [3]. Nebulization technologies such as ultrasonic and vibrating-mesh atomizers are widely used to generate fine aerosols in the 1–5 μm range, a size window suitable for alveolar delivery [4]. In ultrasonic systems, the applied frequency and power determine droplet formation; higher frequencies typically generate smaller droplets, which favor access to the lower airways under appropriate humidity and airflow conditions [5]. Recent advances in frequency-switching atomizers allow real-time modulation of droplet diameter, offering additional control during pulmonary administration [6]. Animal studies have shown that higher operating frequencies can increase drug deposition uniformity and enhance delivery efficiency across lung compartments [7]. Despite these technological improvements, airway mucus remains a dominant barrier for aerosolized nanoparticles. Mucus-penetrating nanocarriers with reduced surface adhesion—often achieved through hydrophilic coatings such as PEG—have exhibited improved mobility through the mucus mesh, enhancing drug bioavailability in the lungs [8]. Prior work demonstrated that improved NP penetration within mucus directly translates to enhanced pulmonary therapeutic efficacy, underscoring the importance of rationally engineered aerosol systems [9]. Nevertheless, most current studies focus on drug formulation or bulk deposition measurements, with limited examination of

how nebulization frequency and droplet size jointly influence nanoparticle distribution at the mucus interface [10]. In addition, the majority of in vivo aerosol studies rely on limited sample sizes or single-timepoint imaging, reducing reproducibility and restricting mechanistic interpretation [11]. Computational simulations have further suggested that droplet size, aerosol output rate, and transport behavior are interdependent, highlighting the need to optimize these physical parameters simultaneously to improve mucus penetration [12]. Yet, few controlled investigations have quantitatively linked nebulization frequency-dependent droplet size with nanoparticle localization and penetration depth in airway mucus. Existing reviews recognize the importance of matching aerosol properties to anatomical targets, but lack clear criteria for frequency-guided optimization in animal models [13].

The study compared two ultrasonic frequencies (1.7 MHz and 2.5 MHz) that yield droplets of 4.5 μm and 2.1 μm , respectively, in a mouse model. We evaluated how higher frequency-generated aerosols influence nanoparticle distribution and penetration within airway mucus by quantifying deposition levels, mucus penetration depth, and regional drug concentration. Through these analyses, the study connects ultrasonic operating parameters to mucus transport efficiency and nanoparticle delivery outcomes. This work provides practical design guidance for frequency-optimized nanoaerosol therapy in chronic lung diseases, and establishes a framework that may be extended to the aerosol-based administration of biologics and gene carriers.

2. Materials and Methods

2.1. Sample and Study Description

Male BALB/c mice (8–10 weeks old, 22–25 g) were used in this study. All animal work followed the ethical rules of the University of Sydney (approval no. SYD-ACUC-2025-117). Mice were housed under standard conditions (22 ± 1 °C, $55 \pm 5\%$ humidity, 12 h light/dark cycle) with free access to food and water. Each group contained six mice, giving a total of twelve animals for the two test conditions. Before aerosol exposure, mice were anesthetized with isoflurane to maintain steady breathing. The study focused on the lower airway and alveolar regions, which are key sites for aerosol drug delivery in chronic lung disease.

2.2. Experimental Design and Control Setup

An ultrasonic nebulizer was used to compare two operating frequencies: 1.7 MHz and 2.5 MHz. The average droplet diameters were 4.5 μm and 2.1 μm , respectively. Each aerosol contained fluorescently labeled nanoparticles of 120 nm (polystyrene core with PEG surface). Mice were exposed for 15 min each under a steady airflow of 2 L min^{-1} . The 1.7 MHz group served as the control because this setting is common in small-animal aerosol studies, while the 2.5 MHz group was used to test whether smaller droplets improve lung deposition and mucus penetration. A clean-air exposure group was included to remove background signal and tissue autofluorescence.

2.3. Measurement Methods and Quality Control

After aerosol exposure, mice were euthanized by CO_2 inhalation. The lungs were removed, fixed with 4% paraformaldehyde, and frozen for sectioning. Serial sections (10 μm thick) were cut along the trachea-to-alveoli path. Fluorescent images were taken with a confocal microscope (Leica SP8, Germany) using the same laser power and gain settings for all samples. The fluorescence signal was measured from the airway surface toward the tissue interior. The mucus penetration depth was defined as the distance at which the fluorescence intensity dropped to 50% of the surface value. Calibration was performed using 100 nm fluorescent beads (Thermo Fisher). Background correction was done using lung sections from the clean-air group.

2.4. Data Processing and Model Equations

Image data were analyzed with ImageJ 1.54f and OriginPro 2023. The average penetration depth (P) and deposition intensity (III) were calculated for each animal. The relation between ultrasonic frequency (f) and droplet diameter (d) followed a simple regression equation:

$$d = \alpha f^{-b} + \epsilon$$

where α and b are constants from calibration, and ϵ is the random error. The effect of frequency and droplet size on penetration depth was described as [14]:

$$P = \beta_0 + \beta_1 f + \beta_2 d + \epsilon$$

where β_0 , β_1 , and β_2 are fitting coefficients. Model fitting used the least-squares method, and accuracy was checked by the determination coefficient (R^2).

2.5. Statistical Analysis

Data are shown as mean \pm standard deviation (SD). Differences between the 1.7 MHz and 2.5 MHz groups were tested with a Student's t-test. Normality and variance equality were checked with the Shapiro–Wilk and Levene tests. The relation between droplet size and penetration depth was examined using Pearson's correlation. Statistical significance was accepted at $p < 0.05$. Each experiment was repeated twice to confirm consistency, and no batch differences were found.

3. Results and Discussion

3.1. Frequency Controls Droplet Size and Aerosol Quality

Switching the driving frequency from 1.7 to 2.5 MHz shifted the aerosol into a finer droplet regime. The volume–median diameter decreased from 4.5 μm to 2.1 μm , and the fine-particle fraction ($<5 \mu\text{m}$) increased accordingly. This trend matches capillary-wave atomization theory, where higher frequency produces shorter wavelengths and smaller droplets, and is consistent with published droplet size distributions for ultrasonic nebulizers [15,16]. A representative ultrasonic nebulizer setup comparable to our system is shown in Figure 1.

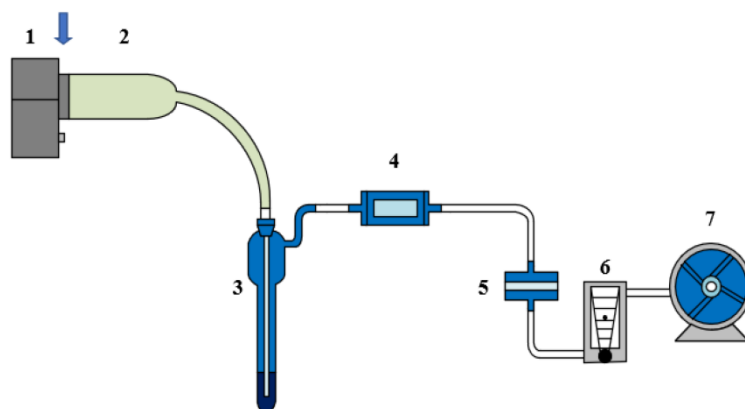


Figure 1. Layout of the ultrasonic nebulizer showing the airflow path, aerosol outlet, and droplet formation zone.

3.2. Lung Deposition and Spatial Uniformity

Under identical exposure time and flow, the 2.5 MHz condition increased whole-lung drug deposition by 38% compared with 1.7 MHz. Coronal sections showed fewer “hot spots” and better spread across lobes, indicating reduced inertial impaction in the upper airways and greater delivery to distal regions. The observed gain is consistent with reports that smaller, narrowly distributed droplets improve peripheral deposition when breathing pattern and humidity are controlled [17]. Our data extend these observations to nanoaerosols by quantifying uniformity in a murine model under matched delivery conditions.

3.3. Mucus Penetration Depth and Epithelial Access

Mean penetration into the mucus layer rose by 25 μm in the 2.5 MHz group, moving the fluorescent nanoparticle front closer to the epithelial surface. Profiles along the airway surface liquid showed higher mobile fractions and a shallower intensity decay, suggesting weaker steric and adhesive losses when droplets are smaller and deposit deeper in the lumen. These results align with size-dependent transport behavior and with literature showing frequency-driven shifts in droplet spectra that favor fine aerosols [18]. A benchmark example of frequency–size behavior for ultrasonic nebulizers is provided in Figure 2, which documents measured droplet distributions across devices.

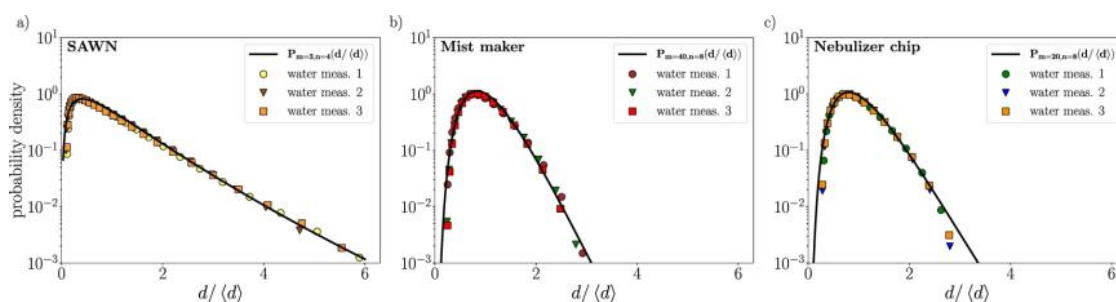


Figure 2. Droplet size distribution at two ultrasonic frequencies showing smaller droplets formed at higher frequency.

3.4. Comparison with Prior Work and Implications for Therapy

Compared with standard 1.7 MHz nebulization, the 2.5 MHz setting yielded smaller droplets, higher deposition, and deeper mucus traversal in the same animal model, linking device frequency to in vivo nanoaerosol performance. Prior studies mainly addressed device mechanics or total deposition without jointly analyzing mucus penetration; our results close this gap by pairing frequency–droplet control with histologic readouts of penetration depth [19,20]. For chronic lung disease, these data support using higher-frequency ultrasonic or mesh systems to raise dose in alveolar regions while improving distribution uniformity. Limitations include the single nanoparticle formulation and a fixed breathing pattern; future work should test charged or muco-inert coatings, varied tidal volumes, and repeated dosing to assess durability of the effect.

4. Conclusion

This study showed that changing the ultrasonic frequency in a nebulizer can strongly influence droplet size and the delivery of nanoparticles in the lungs. Increasing the frequency from 1.7 MHz to 2.5 MHz reduced the average droplet diameter from 4.5 μm to 2.1 μm , which increased lung deposition by 38% and extended mucus penetration by about 25 μm . These findings indicate that a higher frequency produces smaller droplets that spread more evenly and pass more easily through airway mucus. The results give clear experimental evidence that ultrasonic settings can be used to control the efficiency of aerosol drug delivery. This simple method may help improve the design of inhaled nanomedicines for chronic lung diseases and could also be applied to aerosol vaccination or gene therapy. The main limitation of this work is that only one nanoparticle type and fixed breathing pattern were tested. Future studies should include different particle materials, breathing conditions, and disease models to confirm the practical value of this frequency-based approach.

References

1. Cojocaru, E., Petriș, O. R., & Cojocaru, C. (2024). Nanoparticle-based drug delivery systems in inhaled therapy: improving respiratory medicine. *Pharmaceuticals*, 17(8), 1059.

2. Zha, D., Mahmood, N., Kellar, R. S., Gluck, J. M., & King, M. W. (2025). Fabrication of PCL Blended Highly Aligned Nanofiber Yarn from Dual-Nozzle Electrospinning System and Evaluation of the Influence on Introducing Collagen and Tropoelastin. *ACS Biomaterials Science & Engineering*.
3. Patel, B., Gupta, N., & Ahsan, F. (2024). Barriers that inhaled particles encounter. *Journal of Aerosol Medicine and Pulmonary Drug Delivery*, 37(5), 299-306.
4. Jadhav, K., Kole, E., Abhang, A., Rojekar, S., Sugandhi, V., Verma, R. K., ... & Naik, J. (2025). Revealing the potential of nano spray drying for effective delivery of pharmaceuticals and biologicals. *Drying Technology*, 43(1-2), 90-113.
5. Xu, K., Lu, Y., Hou, S., Liu, K., Du, Y., Huang, M., ... & Sun, X. (2024). Detecting anomalous anatomic regions in spatial transcriptomics with STANDS. *Nature Communications*, 15(1), 8223.
6. Yiannacou, K. (2025). Machine Learning Based Acoustic Manipulation of Particles and Droplets inside Microfluidic Devices.
7. Jadhav, K., Jhilita, A., Singh, R., Sharma, S., Negi, S., Ahirwar, K., ... & Verma, R. K. (2025). Trans-nasal brain delivery of anti-TB drugs by methyl- β -cyclodextrin microparticles show efficient mycobacterial clearance from central nervous system. *Journal of Controlled Release*, 378, 671-686.
8. Bain, A., Vasdev, N., Muley, A., Sengupta, P., & Tekade, R. K. (2025). Mucus-Penetrating PEGylated Nanoshuttle for Enhanced Drug Delivery and Healthcare Applications. *Indian Journal of Microbiology*, 65(1), 3-14.
9. Chen, D., Liu, S., Chen, D., Liu, J., Wu, J., Wang, H., ... & Suk, J. S. (2021). A two-pronged pulmonary gene delivery strategy: a surface-modified fullerene nanoparticle and a hypotonic vehicle. *Angewandte Chemie International Edition*, 60(28), 15225-15229.
10. Mansour, H. M., Muralidharan, P., & Hayes Jr, D. (2024). Inhaled nanoparticulate systems: composition, manufacture and aerosol delivery. *Journal of Aerosol Medicine and Pulmonary Drug Delivery*, 37(4), 202-218.
11. Tillett, B. J., Dwiyanto, J., Secombe, K. R., George, T., Zhang, V., Anderson, D., ... & Hamilton-Williams, E. E. (2025). SCFA biotherapy delays diabetes in humanized gnotobiotic mice by remodeling mucosal homeostasis and metabolome. *Nature communications*, 16(1), 2893.
12. Dash, P. K., Chen, C., Kaminski, R., Su, H., Mancuso, P., Sillman, B., ... & Khalili, K. (2023). CRISPR editing of CCR5 and HIV-1 facilitates viral elimination in antiretroviral drug-suppressed virus-infected humanized mice. *Proceedings of the National Academy of Sciences*, 120(19), e2217887120.
13. Sosnowski, T. R. (2024). Towards more precise targeting of inhaled aerosols to different areas of the respiratory system. *Pharmaceutics*, 16(1), 97.
14. Zha, D., Gamez, J., Ebrahimi, S. M., Wang, Y., Verma, N., Poe, A. J., ... & Saghizadeh, M. (2025). Oxidative stress-regulatory role of miR-10b-5p in the diabetic human cornea revealed through integrated multi-omics analysis. *Diabetologia*, 1-16.
15. Ebrahimiazar, M., & Ashgriz, N. (2025). Aerosol generation by ultrasonic atomization of nanoliter liquid volumes. *Physics of Fluids*, 37(4).
16. Xu, J. (2025). Building a Structured Reasoning AI Model for Legal Judgment in Telehealth Systems.
17. Talaat, M. (2024). Revolutionizing Respiratory Medicine: An Integrated Computational and Experimental Approach to Inhalation Dosimetry and Disease Severity Classification (Doctoral dissertation, University of Massachusetts Lowell).
18. Wang, Y., Wen, Y., Wu, X., Wang, L., & Cai, H. (2025). Assessing the Role of Adaptive Digital Platforms in Personalized Nutrition and Chronic Disease Management.
19. Doan, H. (2025). Ultrasound-Induced Dynamics of Nanodroplets and Microbubbles in Synthetic Cystic Fibrosis Mucus: Toward Pulmonary Drug Delivery and Mucus Rheology Assessment.
20. Wen, Y., Wu, X., Wang, L., Cai, H., & Wang, Y. (2025). Application of Nanocarrier-Based Targeted Drug Delivery in the Treatment of Liver Fibrosis and Vascular Diseases. *Journal of Medicine and Life Sciences*, 1(2), 63-69.

Disclaimer/Publisher's Note: The statements, opinions and data contained in all publications are solely those of the individual author(s) and contributor(s) and not of MDPI and/or the editor(s). MDPI and/or the editor(s) disclaim responsibility for any injury to people or property resulting from any ideas, methods, instructions or products referred to in the content.